PAGEOPH, Vol. 139, No. 3/4 (1992)

0033-4553/92/040657-20$1.50 + 0.20/0

Mining-induced Seismicity in Faulted Geologic Structures: An Analysis of Seismicity-induced Slip Potential

P. L. SWANSON[1]

Abstract—Relationships between the locations of mining-induced seismic events, local fault structure, and mine geometry were examined in a deep hard-rock mine in northern Idaho. Stopes experiencing rock bursts and other large seismic events were found to fall into two structural regimes: the "Silver Vein," and the "N48°W Trend," a steeply dipping plane of seismic activity that is subparallel to major local steeply dipping faults which bound blocky structures. The N48°W Trend also intersects a shaft that was seriously damaged when fault gouge was expelled into the opening during a 3-month period of high seismic energy release. Models of stress interaction are used to support the hypothesis that mining-induced deformation was mobilized along a 1.5 km length of the N48°W Trend. Specifically, numerical models are used to simulate rupture of seismic events and estimate induced changes in the quasi-static stress field. A Coulomb failure criterion is used with these results to estimate the spatial variation in potential for slip on planes parallel to local faulting. Increases in the potential for slip on fault planes subparallel to the N48°W Trend are consistent with activation of deformation along its 1.5 km length. For events with constant seismic moment, stress drop is shown to be far more important than source dimension in elevating slip potential along the observed plane of seismic activity.

Key words: Mining-induced seismicity, slip potential, fault-slip, rock bursts, stress interaction.

Introduction

Certain mine geometries and geologic structures play critical roles in the generation of rock bursts and other large mining-induced seismic events (COOK *et al.*, 1966). To develop effective rock burst hazard reduction strategies at a particular mine site, the underlying mechanisms, whether controlled by mine geometry, geology or both, must first be identified. Toward this end, the relationships between large seismic events, mining geometry, and local fault structures are examined in a burst-prone mine in the Coeur d'Alene district of northern Idaho.

Rock bursts in deep hard rock mines have been classified into two groups: those associated with high stresses induced by mine geometry and those linked to interaction of these stresses with preexisting geologic structures such as faults and dykes (e.g., GIBOWICZ, 1990). The high-stress-induced events occurring in the

[1] U.S. Bureau of Mines, Denver Federal Center, Bldg. 20, Denver, CO 80225, U.S.A.

immediate vicinity of mine workings and pillars are often considered to be less damaging (i.e., smaller area of damage) and of lower magnitude than those associated with large-scale slip on faults (GAY *et al.*, 1984; BRUMMER and RORKE, 1990). Nevertheless, fault-slip events can be triggered far out in the host rock without significant, or any, in-mine damage.

Rock bursts in the Coeur d'Alene district are often triggered when mining into remnant (sill) pillars produced by the commonly used overhand cut-and-fill mining method (BLAKE, 1972). In this case both geology and mine geometry influence rock bursting; fault structures are present in the immediate vicinity of mining and they are subjected to high stresses present in the pillars. An attempt to reduce rock bursting by eliminating pillars in an experimental underhand longwall cut-and-fill mining operation is in progress at one mine in the district (WILLIAMS and CUVELIER, 1990). Eliminating pillars, however, does not reduce the frequency of encounters with faults.

This study was initiated after a three-month sequence of large seismic events occurred in six separate production areas (stopes) that fell along a well-defined plane. This 1.5×0.5 km near-vertical plane, hereafter referred to as the N48°W Trend, was generally parallel to the trend of, and approximately coincident with, major local faults. During the same time period, the main entry shaft, which intersects the N48°W Trend, experienced significant ground control problems resulting in a 3-month shutdown. Evidence is presented here that suggests that deformation was mobilized over the entire length of the mine along the N48°W Trend in a series of Richter magnitude (M_L) 2–3 seismic events. A stress-interaction mechanism for this mobilization is investigated.

The paper is organized in the following fashion. First, the structural geology typical of this region is described, followed by descriptions of the stress field and vein geometry. Then, the newly-described N48°W Trend is identified along with other structures known to be associated with rock bursting. The paper then focuses on a short period of high seismic energy release along the N48°W Trend. Using seismic source size and stress-drop estimates and calculations of induced fault-slip potential, a case for stress interaction between these large seismic events is argued.

Structural Geology

The Coeur d'Alene mining district has been described as being located in an intensely faulted and sheared structural knot (HOBBS *et al.*, 1965; WALLACE and MORRIS, 1986). The slightly metamorphosed Precambrian rocks have been compressed into a series of folds with varying amplitudes and wavelengths (synclinorium) and subsequently faulted. Figure 1a shows the portion of the district surrounding the Galena Mine. Two locally dominant structural features, the right-lateral strike-slip Osburn and Placer Creek faults, can be traced for over 100 km

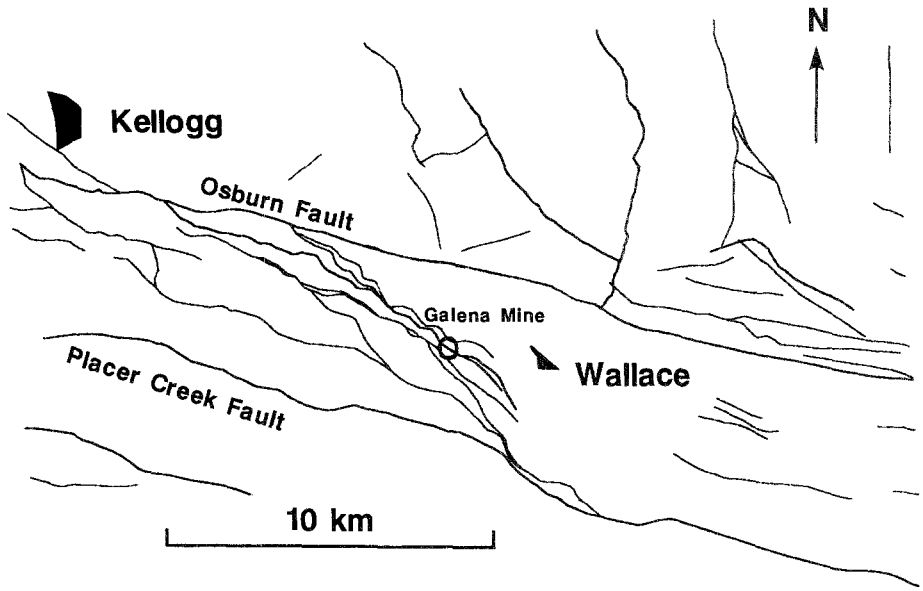

Figure 1(a)

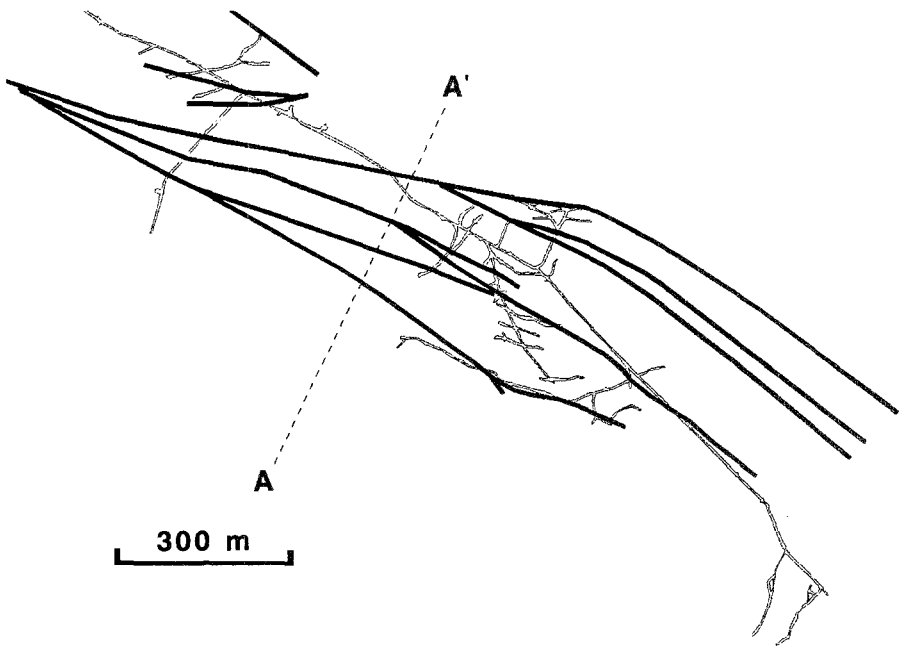

Figure 1(b)

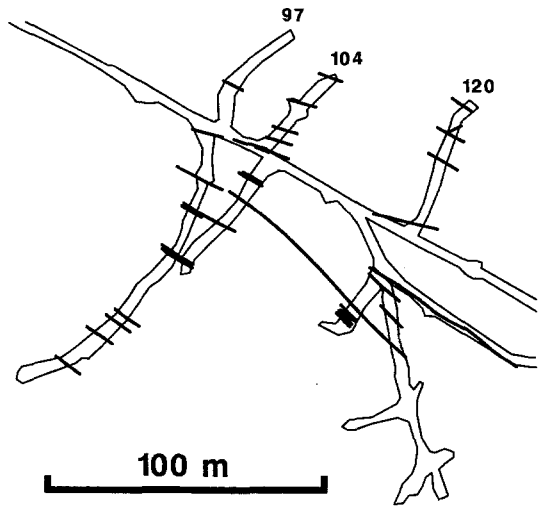

Figure 1(c)

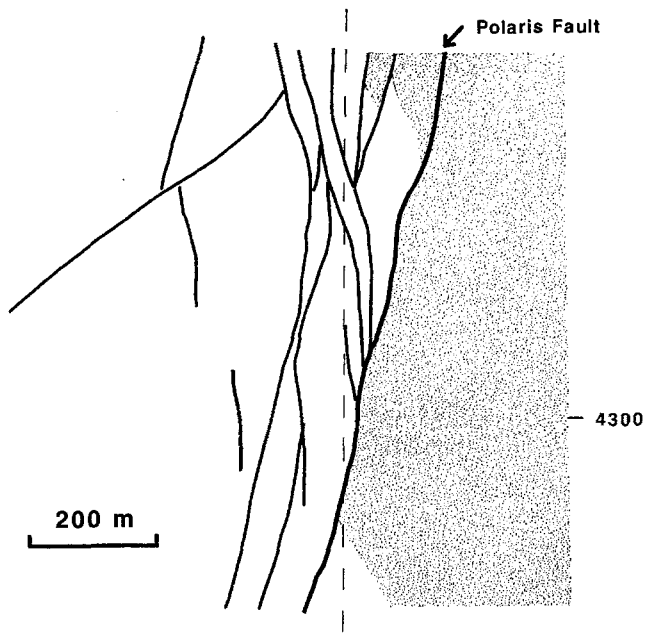

Figure 1(d)

Figure 1

(a) Map view of Silver valley near Galena Mine (open circle) showing major faults, (b) and (c) show finer scales at depth. (d) is vertical cross section through A–A′ in (b). The subset of faults that can be traced between levels and sections is shown in (b) and (d). Shading indicates St. Regis argillites. Dashed line in (d) is trace of N48°W Trend. Mine level is 4300 level.

and make up part of the extensive Lewis and Clark lineament (WALLACE *et al.*, 1980). They are connected via a dense concentration of faults (e.g., Polaris, Silver Standard, Killbuck, Argentine faults) that intersect or occur in the near vicinity of the mine along an approximate N50°–60°W trend. Most of these faults dip steeply to the southwest, and some approach near-vertical in the vicinity of the Galena Mine. Segmentation into complex strands is common.

Figures 1b and c show map views of fault structure at depth. Only faults that can be traced with certainty between mine levels, diamond-drill holes, and sequential vertical cross sections (250 m spacing) are shown in Figure 1b. Many other faults are observed in mine openings (Figure 1c) but, because of their vast numbers and the fact that they can terminate abruptly, they have not been traced between levels. The northwest faulting trend persists down to the scale of a few meters.

The country rock surrounding the mine workings in Figure 1c is the Revette formation. The Revette is locally made up of 0.2 to 1.0 m thick beds of brittle, high strength, high modulus, quartzite that are interbedded with thin beds of argillite (typically <2 cm thick, with rare zones up to 0.7 m). In the vicinity of much of the present mining activity, the beds strike northwest and dip steeply (~ 75–$80°$) to the northeast. Bedding-plane faults are ubiquitous with typical spacing of a few meters. Bedding-plane fault offsets average well under 5 m. Many other faults and joints with various orientations are present, producing a complex blocky structure. Throughout the mine, the maximum size block that is free of visible faults is estimated to be only 5 to 7 m on a side.

Rock bursting is prevalent in the Revette quartzite throughout the Coeur d'Alene district. The Polaris fault separates Revette quartzite from the St. Regis argillites in certain parts of the mine (Figure 1d). A layer of gouge and sheared rock (0.3 to 10.0 m thick with 1.0 m being typical) is commonly observed in mine openings driven through the Polaris fault. Such crossings indicate the weak and highly permeable nature of these larger faults with obvious signs of moisture and enlarged (eroded) mine openings that often need timbered support. Until dried out upon exposure to ventilated mine air, the soft plastic gouge can be molded by hand.

Mine workings that penetrate the Polaris fault, and those located on its St. Regis side, often experience lots of "squeeze" (obvious deformation without significant seismic activity, i.e., $M_L < -1$) and few if any rock bursting problems. Apparently, the St. Regis argillites consume strain energy by deforming plastically, thus reducing the severity of the rock bursting problem.

Faults range from clean and discrete surfaces a few grains in width to the larger shear zones exhibited by the Polaris fault with cataclasis and gouge. In general, fault zones in the quartzite are narrower than in the argillites. The width, however, may depend upon the scale in which the observations are made; a single discrete interface may represent one small facet of a large complex, anastomosing, shear zone involving many structural blocks. The blocky nature of the rock mass found on the scale of individual stopes may be interpreted, in certain instances, as representing deformable elements that belong to much larger fault structures.

In summary, stiff quartzite blocks are bounded by compliant fault structures and argillites and are elongated parallel to these structures. As these structures are commonplace in the Galena Mine, mining-induced deformation may be strongly influenced by rigid-block mechanics.

In Situ Stress and Vein Geometry

Studies of *in situ* stress in the district (BOARD and BEUS, 1984; WHYATT, 1986; SPRENKE *et al.*, 1991) indicate that the dominant direction of maximum horizontal compressive stress is N45°W ± 15°. In the vicinity of the Galena Mine, this direction is parallel to the strike of local faulting and the near-vertical bedding. Limited observations of borehole breakouts in the Galena Mine are consistent with a N45°W maximum principal stress direction. Based on empirical relations fit to *in situ* stress data collected throughout the district (WHYATT, 1986), the vertical, maximum, and minimum horizontal principal stresses in the central part of the mine are estimated to be 38, 51, and 39 MPa, respectively.

All but one of the steeply dipping burst-prone veins strike N35°E to N65°E or roughly perpendicular to both the N48°W Trend and the maximum horizontal-stress direction (see for example veins 97, 104, and 120 in Figure 1c). Faults which intersect these veins range in strike between N45°W and N80°W (e.g., Figure 1b) with most clustering between N50°W and N65°W. Thus the faults generally strike perpendicular to the veins and subparallel to the N48°W Trend.

The vein-normal maximum horizontal stress orientation gives rise to local stress distributions similar to those found in gravity-loaded horizontal tabular deposits with large end lobes of high shear stress (e.g., JAEGER and COOK, 1976). Alignment of the high shear stress lobes with the preexisting fault surfaces and argillite (and other) bedding planes provides optimum conditions for aiding stope closure through both stable and unstable right-lateral and left-lateral slip.

Spatial Distribution of Rock Bursts

At a depth of 1.0 to 1.7 km, the silver ore vein deposits of the Galena Mine are extracted using the overhand cut-and-fill method. There are more than 40 near-vertical veins that are distributed, in subparallel fashion, over a horizontal distance of 1.5 km. Approximately 20 different stopes are mined at any one time. Of these, ten may be prone to rock bursting.

The seismicity data described in this paper was initially examined in order to constrain the design of a full seismic waveform recording system; thus, source mechanism analyses are not available. Richter magnitudes were estimated from a calibrated short-period vertical seismometer on the surface. Events were located

(SWANSON and SINES, 1991) using one of eight 16-channel accelerometer arrays in a networked microseismic monitoring system (STEBLAY *et al.*, 1990). This system provides real-time hypocenter locations for events with magnitudes greater than -5. Each array is approximately 150 m on a side and is centered around individual rock-burst-prone stopes. Location errors for events falling within an individual array, where the detection and location sensitivity are greatest, are ± 10 m at best (SWANSON *et al.*, 1993).

Approximately 200 of the largest mining-induced seismic events with M_L ranging from 0.0 to $+3.0$ were located. Figure 2 shows a histogram of all located seismic events and the subset of damaging seismic events. A damaging seismic event is defined here as one which requires at least one-half day of clean up and/or repair.

Ten rock-burst-prone stopes were observed to fall into two different structural regimes: the "Silver Vein" and the N48°W Trend (Figure 3). The map view shown

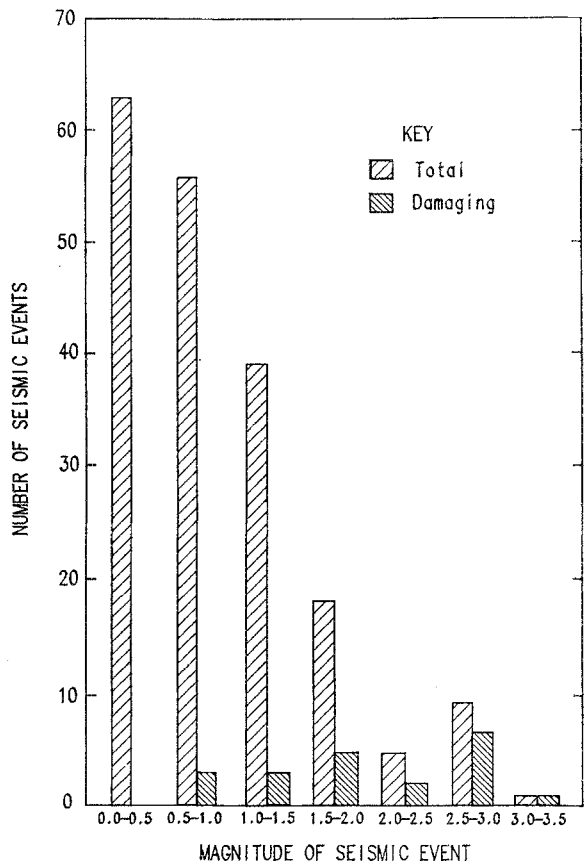

Figure 2
Distribution of event magnitudes for time period January 1989 through June 1991.

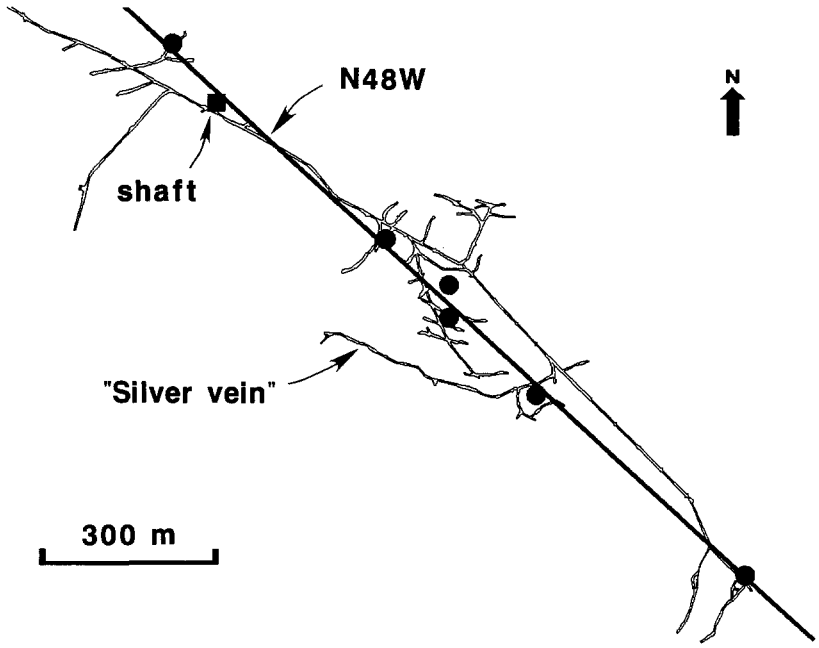

Figure 3
N48°W Trend of stopes (solid circles) experiencing rock bursting and other large seismic events, and damaged shaft. Rock-burst-prone stopes of the Silver Vein are omitted for clarity. Plan view shows 4300 level at 1.3 km depth.

in Figure 3 illustrates the two structural regimes and the 4300 level at approximately 1.3 km depth. The Silver Vein is the largest vein in the mine and has been associated with rock bursts since the 1950s. It extends at least 1 km vertically and as much as 400 m horizontally. The mined horizontal extent of more typical veins is 80 to 120 m. The near-vertical veins have a height that is typically 2–4 times their breadth with an excavation width of 2–5 m.

Six stopes with recurring seismic activity plus the damaged shaft define the N48°W Trend. In one 11-month period, 30 of 32 events detected with $M_L > 1.0$ occurred exclusively along the N48°W Trend despite the fact that mining was progressing in at least 25 different stope and development headings that were not on this alignment. Several particularly large seismic events ($M_L > 2.5$) occurred in the last three months of this 11-month period. The remainder of the paper focusses on this short period of high seismic activity along the N48°W Trend.

Concentrated Release of Seismic Energy

Periods of elevated rock burst activity or rock burst "seasons" have long been recognized by old-time Galena miners. One such period of elevated activity oc-

curred in the first three-months of 1990 (Figure 4). Over ninety percent of the seismic energy released from the mine in 1990 was released in this time period. Seismic energy E (ergs) was estimated using GUTENBERG and RICHTER's (1956) relation $\log E = 11.8 + 1.5M$ with M_L as magnitude M. The seismic energy emitted from the N48°W Trend occurred in a series of 11 events with $M_L = 1.1$ to 2.9. Four events ranging from $M_L = 2.6$ to 2.9 dominate the periods of energy release labelled, a, b, d, and e in Figure 4. The main entry shaft damage at "c" occurred shortly after the largest event of the sequence at "b." Following the short period of high seismic energy release the rate remained below the average long-term rate, indicated by slope of dashed line in Figure 4, for 10 months. Mining productivity was nearly constant during this entire time period.

The temporal coincidence of a rapid sequence of large seismic events and shaft damage (all occurring on the N48°W Trend), followed by a significant quiet period, is suggestive of large-scale release of stored elastic strain energy through activation of fault slip along one of the major northwest trending fault structures. However, a single major discontinuity surface cannot be traced through the N48°W Trend. It should be re-emphasized that faults on the scale of the mine in the Coeur d'Alene district are not simple planar structures but are complex, multiple, anastomosing surfaces that can vary rapidly in character over very short distances (WALLACE and

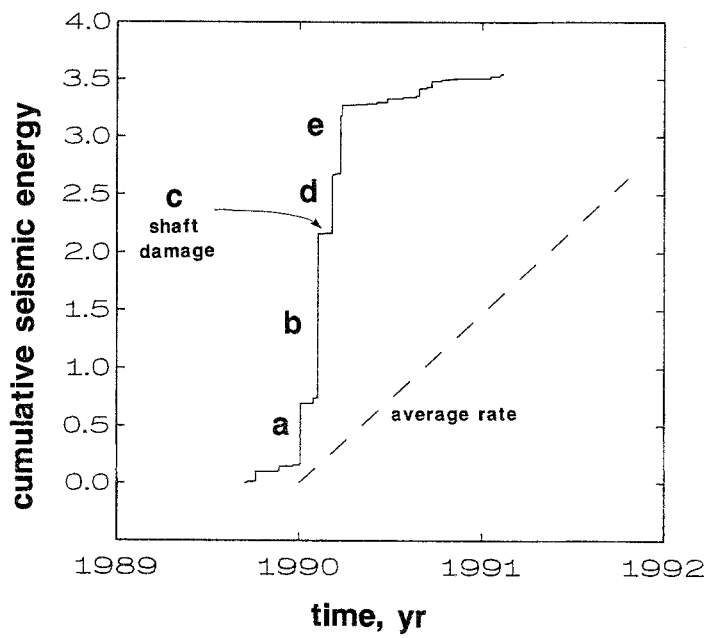

Figure 4
Cumulative seismic energy (units of GJ) released along N48°W Trend. Periods of energy release a, b, d, e are associated with events shown in Figure 7. c denotes time of fault-gouge expulsion into main entry shaft. Dashed line shows long-term average energy release rate.

MORRIS, 1986). Therefore, even if one envisaged a complex three-month long propagation of a shear slip event that was periodically triggered by mining activity, the presence of a single continuous discontinuity surface does not seem to be required for fault structure and movement on this scale. An alternative interpretation involves the transmission of seismicity-induced changes in stress by relatively rigid quartzite blocks that are elongated parallel to the dominant northwest fault structures. The latter view is consistent with the expected mechanical response of the local geologic structure.

Relationship Between Source Size and Event Magnitude

An approximate measure of the rupture size for the events of Figure 4 is required in order to evaluate the degree to which ruptures initiating in a particular stope affect the stress field in adjacent stopes. Such interaction may promote stope closure and release of stored energy along the N48°W Trend.

Figure 5 shows a compilation of published estimates of source dimensions for mining-induced events of a given seismic moment M_0. These estimates assume a shear dislocation source for which a Brune model (BRUNE, 1970) applies. As source

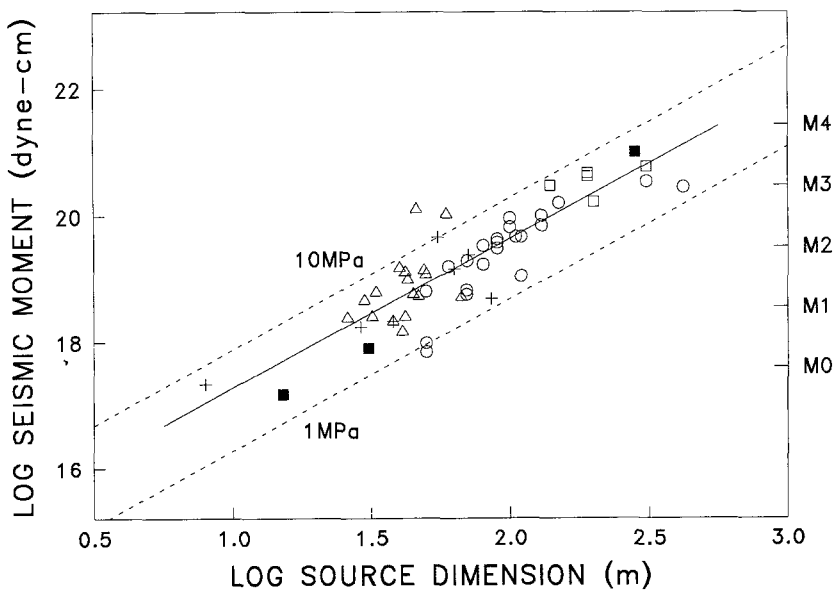

Figure 5

Seismic moment source dimension relations from Brune model applied to mining-induced events (○—SPOTTISWOODE and MCGARR, 1975; + —MCGARR *et al.*, 1981; △—SPOTTISWOODE, 1984; ■—MCGARR *et al.*, 1990). Dashed lines show lines of constant stress drop (1, 10 MPa). Solid line (2.2 MPa) represents fit to data.

dimension estimates are model dependent, comparisons are restricted to data analyzed with the Brune model. Reported values of source dimension r and stress drop $\Delta\tau_0$ correspond to homogeneous faulting models. Variation of source size, for a given moment, reflects differing stress drops, asssuming all other sources of variation, such as attenuation, are identified.

A linear fit to the data at 95% confidence,

$$\log M_0(\text{dyne-cm}) = (2.9 \pm 0.6) * \log r(\text{m}) + (13.8 \pm 1.1) \quad (1)$$

is shown as a solid line in Figure 5. For the range of source dimensions shown ($\sim$10 to 300 m), the data is consistent with a constant stress-drop trend. The stress drop associated with the fitted line is 2.2 MPa.

The empirical relationship,

$$\log M_0 = 1.2 * M_L + 17 \quad (2)$$

determined for small central California earthquakes in the magnitude range $1.5 \leqq M_L \leqq 3.5$ (BAKUN, 1984), and equation (1) were used to estimate source dimensions from magnitude.

As a check on the assumed relationship between magnitude and source dimension, the mine volume exhibiting microseismicity ($M_L \geqq -5$) following a M_L 2.9 event was estimated using the data from the microseismicity monitoring system. The event occurred in the country rock between the stopes covered by four separate arrays of the monitoring system (Figure 6). Damage was restricted to rock falls on several levels, and one M_L 0.9 aftershock on the 4300 level uplifted a train track a few centimeters. The observed volume of aftershock microseismicity is a minimum due to the extremely low detection sensitivity outside of individual accelerometer arrays. Nearly 4000 microseismic events were detected during the 10.5 hours following the M_L 2.9 event. Less than 700 events were actually located; the remainder did not meet the location criteria used in the routine monitoring system (SWANSON *et al.*, 1993). An order of magnitude fewer events are typically located with these four arrays during the same time period on days with no large rock bursts. Included in Figure 6 is a Brune model representation of the seismic source estimated from Figure 5 ($r = 201$ m). Both estimates of source dimension (Figures 5 and 6) are of the same order of magnitude.

Hypothesis: Mobilization of Deformation Along Length of Mine

The average relationship between magnitude and source size (equations (1) and (2)) is now used to illustrate the fraction of the N48°W Trend which could be occupied by slipped area if all the events had a N48°W orientation. The case for

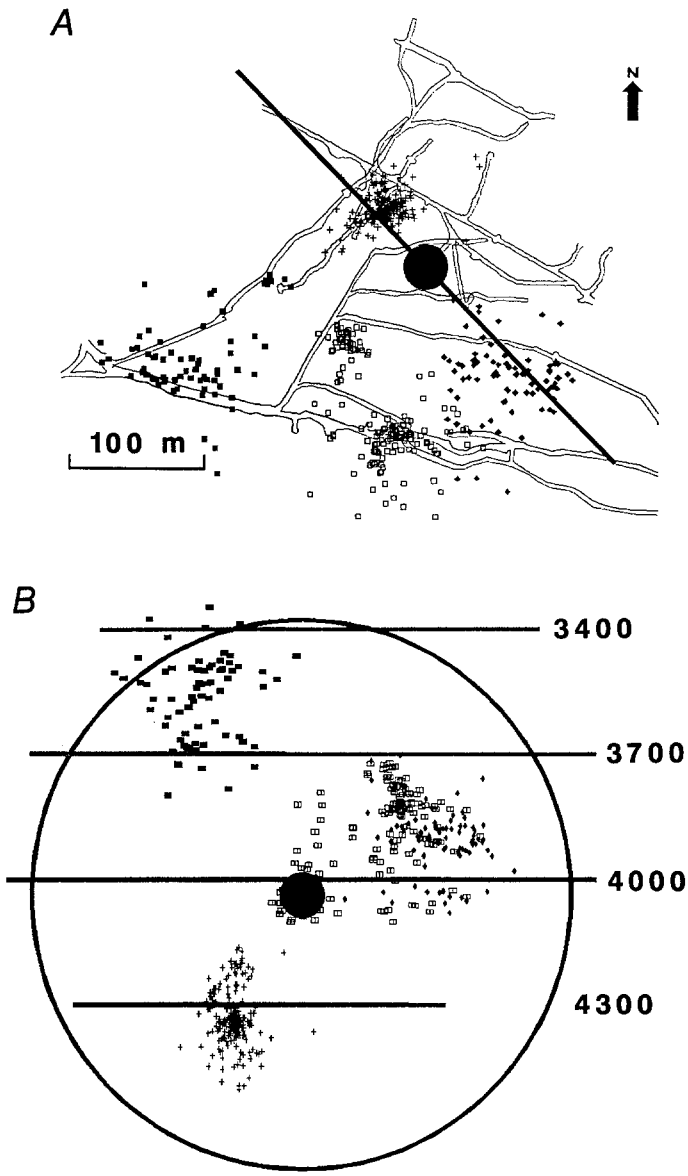

Figure 6

Source dimension estimate for M_L 2.9 event based on volume distribution of microseismicity recorded for 10.5 hours by four arrays of the networked monitoring system. Hypocenter is shown as large solid dot. Hypocenter location uncertainty is ± 40 m. Apparent clustering is due largely to low detection sensitivity in regions between the four arrays. Source dimension estimate from equations (1) and (2) shown as a 201 m radius circle in (A) plan view, and (B) vertical section looking northeast.

making this assumption rests not on hard data, i.e. event mechanisms, but rather on the structural geology, the compatibility of N48°W slip with stope closure, and the observed event alignment. Figure 7 shows a vertical section of the plane of induced seismic activity (looking northeast). Estimated sizes and positions of rupture planes correspond to individual events ($M > 1$) occurring during the periods of energy release (a–e) shown in Figure 4. A significant fraction of the 1.5 × 0.5 km plane of seismic activity is covered by the circular rupture sources.

To investigate the degree of stress interaction between these events, elementary two-dimensional elastic stress analyses were used to calculate quasi-static stress changes due to simple shear rupture sources. In particular, the increase in the potential for slip along the N48°W Trend due to double-couple sources at other positions on this plane is examined. Slip potential, in this usage, describes the difference between the shear stress, τ, acting on a plane and the Coulomb shear stress condition for failure on that plane (e.g., JAEGER and COOK, 1976),

$$\text{slip potential} = |\tau| - s_0 - \mu(\sigma_n - p), \tag{3}$$

where s_0 is the cohesive shear strength, μ is the coefficient of friction (or internal friction for intact rock), σ_n is the normal stress across the plane, and p is pore fluid pressure. Equation (3) is identical to the excess shear stress (ESS) parameter of RYDER (1988) and others, that expresses the difference between static shear stress prior to slip and the dynamic strength of the plane, when μ is the dynamic coefficient of friction and $p = 0$. To avoid de-emphasizing the influences of normal stress and pore fluid pressure on the potential for quasi-static creep and/or dynamic shear slip, the terms slip potential and/or Coulomb failure function (OPPENHEIMER et al., 1988; REASENBERG and SIMPSON, 1992) are used here.

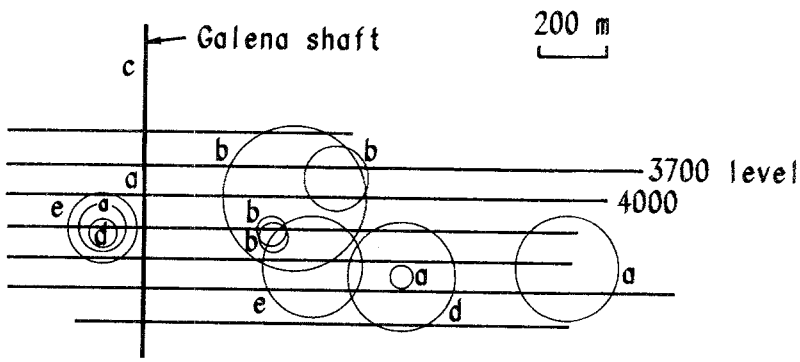

Figure 7
Vertical section view of N48°W plane of seismic activity (looking northeast). Estimated sizes and positions of circular rupture planes correspond to periods of energy release (a–e) shown in Figure 4. The Galena shaft (c) is shown as a black vertical line.

When geologic and/or mine structures are stressed close to failure, arbitrarily small perturbations in the stress field may trigger instability. The change in the potential for slip (e.g., ΔCFF, REASENBERG and SIMPSON, 1992) due to stress altering events is given by (e.g., OPPENHEIMER *et al.*, 1988 and others)

$$\Delta(\text{slip potential}) = \Delta\tau + \mu(\Delta\sigma_n - \Delta p), \tag{4}$$

where $\Delta\tau$ is the change in shear stress, $\Delta\sigma_n$ is the change in normal stress (positive for increased tension), and Δp is the change in pore pressure. No changes are assumed to occur in s_0 and μ.

Stress changes associated with the first three events in the sequence of Figure 7 (label "a") are estimated. These events occurred within a 24-hour period. The boundary element method of CROUCH and STARFIELD (1983) was employed with a modification to maintain contact between crack surfaces. The ruptures are represented by elements placed at each event location and oriented N48°W. Rupture dimensions are scaled by the appropriate event magnitude. A right-lateral shear stress of 2.2 MPa, corresponding to the stress drop determined from the fit to seismic data in Figure 5, is applied across each slip plane and field stresses are calculated. μ and s_0 are taken to be 0.6 and 0.3 MPa, respectively. Pore-pressure effects are neglected.

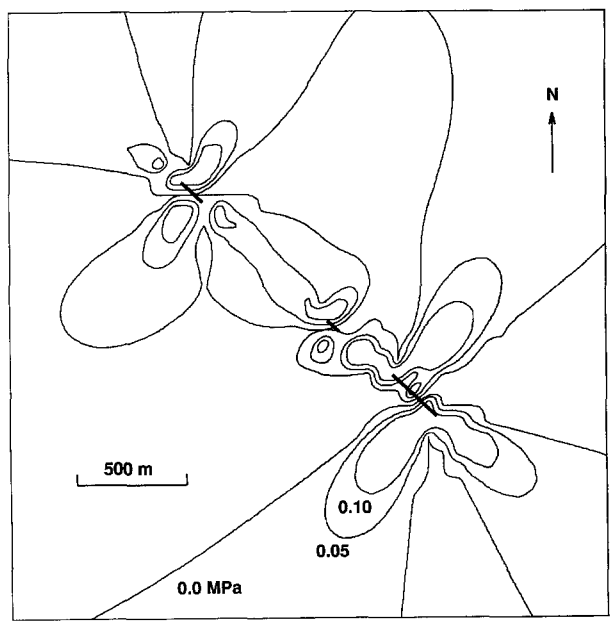

Figure 8
Plan view map showing boundary element model of the first three ruptures (dark lines) in sequence "a" of Figure 7 (from upper left to lower right M_L = 1.8, 1.1, and 2.6). Contours indicate values of increased slip potential (MPa) for N48°W-oriented planes as a result of 2.2 MPa right-lateral stress drops across the three ruptures.

A homogeneous isotropic medium is first considered for simplicity. This neglects two influences. First, a nonuniform stress distribution is expected in a deforming faulted block medium. However, currently, there is not sufficient information to determine which of the ubiquitous potential slip planes should be included in a tractable model. Appropriate constitutive relations and initial boundary conditions are also unknown. Secondly, the stress concentrating effect of the stope geometry is neglected. In these initial calculations, the intent is to estimate the distance over which significant stress changes occur due to simple rupture sources. Neglect of the lower elastic modulus of the sandfill in adjacent stopes results in lower bound estimates of induced stress.

Figure 8 shows the resulting contours of increased slip potential for planes oriented N48°W. A band of elevated slip potential encompasses the N48°W Trend and beyond. Similar results are found for planes oriented parallel to the strike of most major faults (N45°W to N65°W) near the stopes along the N48°W Trend. When the stress drops for the three events do not all have the same sign, slip potential along the N48°W Trend is decreased relative to Figure 8.

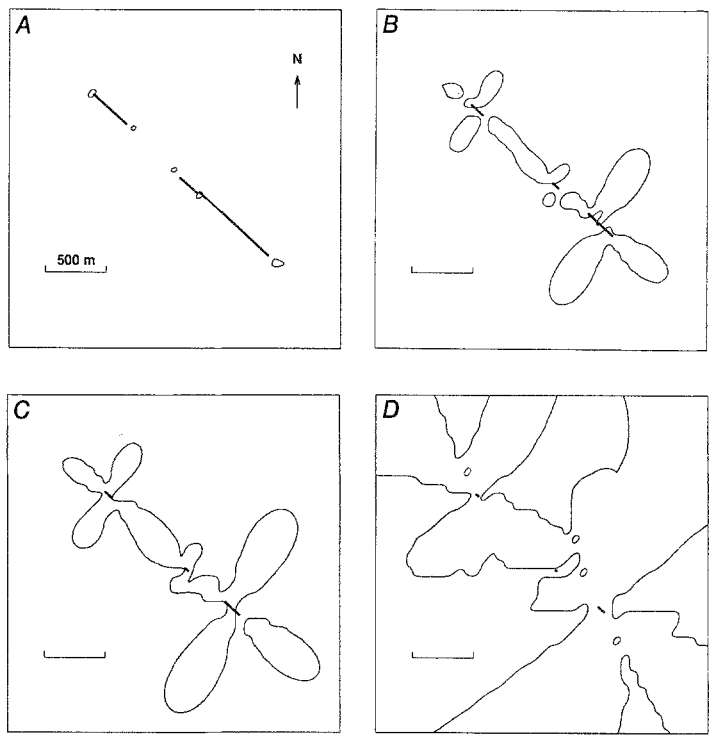

Figure 9
Plan view map of 0.05 MPa (0.5 bar) slip-potential contours for N48°W-oriented planes as a result of (A) 0.1, (B) 2.2, (C) 10.0, and (D) 100.0 MPa right-lateral stress drops across the three ruptures.

The degree to which the results of Figure 8 depend upon the particular combination of source dimension and stress drop was investigated. As seismic moment scales as the product of r^3 and $\Delta\tau_0$ in the Brune model (BRUNE, 1970), specification of one of these parameters allows calculation of the other for a given seismic moment. Additional stress drop values of 0.1, 10, and 100 MPa were used with the seismic moments assumed for the three events in Figure 8 to calculate corresponding source dimensions. These source-dimension/stress-drop combinations were then used to calculate the +0.05 MPa (0.5 bar) slip potential contours shown in Figure 9. The results of Figure 8 ($\Delta\tau_0 = 2.2$ MPa) are included for comparison. Figure 9 indicates that, for a given seismic moment, higher values of stress drop result in greater slip potential in the areas between, and adjacent to, stopes even though the corresponding source dimensions are smaller. Furthermore, stress drops as small as 0.1 MPa would not be expected to result in significant stress interaction along the N48°W Trend.

Discussion

In recent studies, small increases in slip potential have been associated with triggering seismic and aseismic crustal deformation. Increases in slip potential greater than 0.01 MPa have been identified with zones of aftershocks triggered by crustal near-vertical strike-slip faults (OPPENHEIMER *et al.*, 1988; REASENBERG and SIMPSON, 1992; STEIN *et al.*, 1992). Correlations between aftershock locations and increases in the Coulomb failure function of >0.3 MPa have been found in studies of similar events by STEIN and LISOWSKI (1983). Similarly small values are suggested for triggering reservoir-induced seismicity (GRASSO, 1983; ROELOFFS, 1983) and tidally triggered deep lunar seismicity (TOKSÖZ *et al.*, 1977). Fault creep, which is one interpretation of the event producing the shaft damage, has also been observed to be accelerated by changes in slip potential of a few tenths of a MPa (SIMPSON *et al.*, 1988).

Small stress changes that trigger local instabilities in the Galena Mine have long been inferred from observations of (i) microseismic activity occurring several hundred meters from, but concurrent with, small volume (~ 10 m^3) production blasting, (ii) rock bursts and other large seismic events which are occasionally triggered at significant distances from, but concurrent with, blasting (~ 100 m), and (iii) the high occurrence rates of seismic doublets or pairs of events in space and time (SWANSON and SINES, 1990). The values of increased slip potential in Figure 8 are of the same order of magnitude or larger than those reported in the above-mentioned field studies and cover multiple stopes along the N48°W Trend. Similar results are found in models of the other large events in Figure 7. We take this as evidence to support the idea that seismicity- and blasting-induced quasi-static stress changes may link deformation of highly stressed areas over the observed distances.

As shown in Figure 9, the area in which such linked deformation is likely is increased when stress drops are high.

Similarity of focal mechanisms is not a requirement for triggered slip in adjacent working areas; the mechanism need only be such as to accommodate stope closure. (This is at least the case when stress due to closure in a pre-existing stress field is the local dominant force driving the rock bursts/seismic events. This may not be the case for tectonically driven events triggered by mining.) Each stope has elevated slip potential for both left- and right-lateral strike slip. For example, Figure 10 schematically shows one stope intersecting the N48°W Trend at nearly 90 degrees. Absolute values of slip potential are shown for slip on N48°W planes. The direction of σ_1 in Figure 10 was taken to be N30°W, representing one end of the reported range of the maximum principal stress direction (N45°W $\pm$15°). Symmetry of contour lobe size and orientation occurs with σ_1 oriented at N45°W. The elevated slip potential lobes are thus elongated to the northwest over the reported range of σ_1 orientation. Local fault structures (Figure 1) and bedding planes parallel to these elevated slip-potential lobes are candidates for seismic and aseismic slip (both right- and left-lateral).

Model results shown in Figure 10 apply to an isolated stope. Preliminary modeling efforts, in which seismic slip surfaces and multiple mine openings are

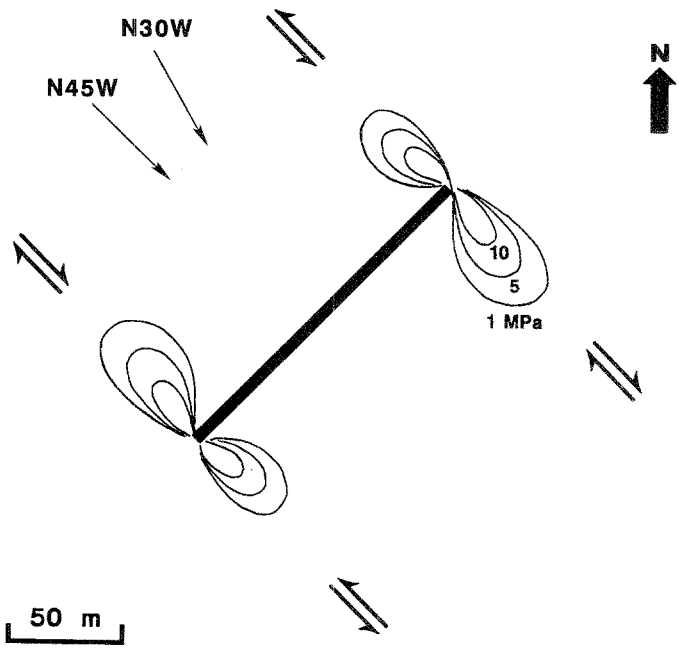

Figure 10
Absolute slip-potential contours (MPa) for slip on N48°W-oriented planes near isolated stope on N48°W Trend (plan view). Contours calculated for N30°W stress direction. Perfect contour symmetry occurs for σ_1 oriented at N45°W.

considered together, indicate that (i) significant interaction between the stopes occurs under static nonseismic loading conditions, (ii) N48°W-oriented seismic events further perturb the slip potential throughout multiple stopes along the N48°W Trend, and (iii) the change in slip potential may be positive or negative depending upon the relative orientations of the slip plane, slip direction, and strike of the stope (vein) and the relative positions of the slip plane and stope. Such perturbation of slip potential represents one possible mechanism by which deformation may be mobilized in multiple working areas throughout the mine.

The evidence presented to support the hypothesis that mining-induced deformation was mobilized along the entire length of the mine cannot be considered unequivocal proof of the hypothesis. It can be argued, however, that it is reasonable, the evidence is consistent, and these results deserve further consideration in development of hazard forecasting and destressing methods in mines with similar conditions.

Summary

The relationship between local geology, vein/stope layout, and the locations of large seismic events and rock bursts has been examined in a deep hard-rock mine in northern Idaho. Two structural regimes were found to be associated with rock bursting: (i) the Silver Vein, the largest vein in the mine with a long history of rock bursting, and (ii) the N48°W Trend, a near-vertical plane striking N48°W throughout the length of the mine. This plane is subparallel to the strikes of the major faults in the mine.

Over ninety percent of the seismic energy emanating from the mine in 1990 was released in one three-month period in a series of large seismic events and rock bursts along the N48°W Trend. During this time, the main access shaft, which is coincident with the N48°W Trend, was damaged when fault gouge was expelled into the shaft opening. While a single discrete fault surface cannot be traced continuously throughout the length of the plane of activity, steeply dipping fault structures trending N45°W to N70°W permeate the mine. These blocky structures are thought to provide preferential slip surfaces to aid stope closure and to facilitate stress transfer between adjacent working areas.

The degree to which Brune-type slip surfaces fill the N48°W plane of activity was examined using published relationships between seismic moment and source dimension. Boundary element models of simple double-couple slip were utilized to estimate quasi-static stress changes associated with three seismic events initiating the rapid period of energy release. Attendant changes in slip potential for planes parallel to fault structures were calculated using a range of stress-drop/source-dimension combinations. For a given seismic moment, stress drop is far more effective than rupture dimension in elevating slip potential along the observed plane

of seismic activity. For stress drops greater than or approximately equal to 2.2 MPa (the average of published results), a zone of elevated slip potential extends along the entire N48°W Trend with values approaching and exceeding those reported for triggering moderate strike-slip earthquake aftershock activity, fault creep, and reservoir-induced seismicity. The evidence presented supports the hypothesis that mining-induced deformation was mobilized along the N48°W Trend throughout the mine.

Acknowledgments

The author thanks ASARCO Inc. for their cooperation with the Bureau in the field experiments at the Galena Mine. Mine geologists J. Lucini and H. Lenhardt contributed substantially to the author's understanding of Coeur d'Alene geology. J. Whyatt (Bureau of Mines, Spokane) provided the modified boundary element code and instruction in its use. Significant improvements were made to the manuscript following reviews by F. Boler, B. Kranz, I. Wong, K. Zipf, and an anonymous reviewer.

REFERENCES

BAKUN, W. H. (1984), *Seismic Moments, Local Magnitudes, and Coda-duration Magnitudes for Earthquakes in Central California*, Bull. Seismol. Soc. Am. *74*, 439–458.

BLAKE, W. (1972), *Rock Burst Mechanics*, Quart. Colo. School of Mines *67*, 1–64.

BOARD, M., and BEUS, M., *Instrumentation and Preliminary Analysis of a 6,200-ft Deep Circular Shaft in Northern Idaho*, Geomechanics Applications in Underground Hardrock Mining (Proc. Soc. Mining Engineers, Denver, 1984), AIME, 127–140.

BRUMMER, R. K. and RORKE, A. J., *Case studies on large rockbursts in South African gold mines.* In *Rockbursts and Seismicity in Mines* (Proc. 2nd Int. Symp. Rockbursts and Seismicity in Mines, Minneapolis, MN, June 8–10, 1988) (Balkema, Rotterdam 1990) pp. 323–329.

BRUNE, J. N. (1970), *Tectonic Stress and the Spectra of Seismic Shear Waves from Earthquakes*, J. Geophys. Res. *75*, 4997–5009.

COOK, N. G. W. (1963), *The seismic location of rockbursts.* In Proc. 5th U.S. Nat. Symp. on *Rock Mechanics*, pp. 493–516.

COOK, N. G. W., HOEK, E., PRETORIUS, J. P. G., ORTLEPP, W. D., and SALAMON, M. D. G. (1966), *Rock Mechanics Applied to the Study of Rockbursts*, J. S. Afr. Inst. Min. Metall. *66*, 436–528.

CROUCH, S. L., and STARFIELD, A. M., *Boundary Elements in Solid Mechanics* (Allen and Unwin, London 1983) 322 pp.

ESTEY, L. H., SWANSON, P. L, BOLER, F. M., and BILLINGTON, S., *Microseismic source locations: A test of faith.* In *Rock Mechanics Contributions and Challenges* (Proc. 31st U.S. Nat. Symp. on Rock Mechanics, Golden, CO, June 1990) (Balkema, Rotterdam 1990) pp. 939–946.

GAY, N. C., SPENCER, D., VAN WYK, J. J., and VAN DER HEEVER, P. K., *The control of geological and mining parameters on seismicity in the Klerksdorp gold mining district.* In Proc. *1st Int. Congr. on Rockbursts and Seismicity in Mines, 1984* (SAIMM, Johannesburg 1984) pp. 107–120.

GIBOWICZ, S. J. (1990), *The mechanism of seismic events induced by mining: A review.* In *Rockbursts and Seismicity in Mines* (Proc. 2nd Int. Symp. Rockbursts and Seismicity in Mines, Minneapolis, MN, June 8–10, 1988) (Balkema, Rotterdam 1990) pp. 3–27.

GRASSO, J. R. (1993), *Mechanics of Seismic Instabilities Induced by the Recovery of Hydrocarbons*, Pure Appl. Geophys. *139*, 507–534.

GUTENBERG, B., and RICHTER, C. F. (1956), *Magnitude and Energy of Earthquakes*, Ann. Geofis. *9*, 1–15.

HOBBS, S. W., GRIGGS, A. B., WALLACE, R. E., and CAMPBELL, A. B. (1965), *Geology of the Coeur d'Alene District, Shoshone County, Idaho*, U.S. Geol. Surv. Prof. Paper *478*, 139 pp.

JAEGER, J. C., and COOK, N. G. W., *Fundamentals of Rock Mechanics* (Chapman and Hall, NY 1976) 585 pp.

MCGARR, A., BICKNELL, J., CHURCHER, J., and SPOTTISWOODE, S. (1990), *Comparison of Ground Motion from Tremors and Explosions in Deep Gold Mines*, J. Geophys. Res. *95*, 21,777–21,792.

MCGARR, A., GREEN, R. W. E., and SPOTTISWOODE, S. M. (1981), *Strong Motion of Mine Tremors: Some Implications for Near-source Ground Motion Parameters*, Bull. Seismol. Soc. Am. *71*, 295–320.

OPPENHEIMER, D. H., REASENBERG, P. A., and SIMPSON, R. W. (1988), *Fault Plane Solutions for the 1984 Morgan Hill, California, Earthquake Sequence: Evidence for the State of Stress on the Calaveras Fault*, J. Geophys. Res. *93* (B8), 9007–9026.

REASENBERG, P. A., and SIMPSON, R. W. (1992), *Response of Regional Seismicity to the Static Stress Change Produced by the Loma Prieta Earthquake*, Science *255*, 1687–1690.

ROELOFFS, E. (1993), *Can Poroelastic Models Explain the Focal Mechanisms of Reservoir-induced Seismicity?* Pure Appl. Geophys., in preparation.

RYDER, J. A. (1988), *Excess Shear Stress in the Assessment of Geologically Hazardous Situations*, J. S. Afr. Inst. Min. Metall. *88* (1), 27–39.

SIMPSON, R. W., SCHULZ, S. S., DIETZ, L. D., and BURFORD, R. O. (1988), *The Response of Creeping Parts of the San Andreas Fault to Earthquakes on Nearby Faults: Two Examples*, Pure Appl. Geophys. *126*, 665–685.

SPOTTISWOODE, S. M., *Source mechanisms of mine tremors at Blyvooruitzicht gold mine.* In Proc. *1st Int. Congr. on Rockbursts and Seismicity in Mines, 1984* (SAIMM, Johannesburg 1984) pp. 107–120.

SPOTTISWOODE, S. M., and MCGARR, A. (1975), *Source Parameters of Tremors in a Deep-level Gold Mine*, Bull. Seismol. Soc. Am. *65*, 93–112.

SPRENKE, K. F., STICKNEY, M. C., DODGE, D. A., and HAMMOND, W. R. (1991), *Seismicity and Tectonic Stress in the Coeur d'Alene Mining District*, Bull. Seismol. Soc. Am. *81*, 1145–1156.

STEBLAY, B. J., SWENDSEID, J., and BRADY, B., *Innovative microseismic rock burst monitoring system.* In *Rockbursts and Seismicity in Mines* (Proc. 2nd Int. Symp. Rockbursts and Seismicity in Mines, Minneapolis, MN, June 8–10, 1988) (Balkema, Rotterdam 1990) pp. 259–262.

STEIN, R. S., KING, G. C. P., and LIN, J. (1992), *Change in Failure Stress on the Southern San Andreas Fault System Caused by the 1992 Magnitude = 7.4 Landers Earthquake*, Nature *258*, 1328–1332.

STEIN, R. S., and LISOWSKI, M. (1983), *The 1979 Homestead Valley Earthquake Sequence, California: Control of Aftershocks and Postseismic Deformation*, J. Geophys. Res. *88* (B8), 6477–6490.

SWANSON, P. L., ESTEY, L. H., BOLER, F. M., and BILLINGTON, S. (1993), *Mining-induced Microseismic Event Location Errors: Accuracy and Precision of Two Location Systems*, Pure Appl. Geophys. *139*, 375–404.

SWANSON, P. L., and SINES, C. D. (1990), *Repetitive Seismicity and Rock Bursting along a Plane Parallel to Known Faulting in the Coeur d'Alene District, ID*, Trans. Am. Geophys. Un., EOS *71*, 1453 pp.

SWANSON, P. L., and SINES, C. D. (1991), *Characteristics of Mining-induced Seismicity and Rock Bursting in a Deep Hard-rock Mine.* Bur. of Mines Report of Invest. 9393, 12 pp.

TOKSÖZ, M. N., GOINS, N. R., and CHENG, C. H. (1977), *Moonquakes: Mechanisms and Relation to Tidal Stresses*, Science *196*, 979–981.

WALLACE, C. A., LIDKE, D. J., and SCHMIDT, R. G. (1990), *Faults of the Central Part of the Lewis and Clark Line and Fragmentation of the Late Cretaceous Foreland Basin in West-central Montana*, Geolog. Soc. Am. Bull. *102*, 1021–1037.

WALLACE, R. E., and MORRIS, H. T. (1986), *Characteristics of Faults and Shear Zones in Deep Mines*, Pure Appl. Geophys. *124*, 107–125.

WHYATT, J. K. (1986), *Geomechanics of the Caladay Shaft*, M.S. Thesis, Univ. of Idaho, Moscow, ID.

WILLIAMS, T. J., and CUVELIER, D. J., *Report on a field trial of an underhand longwall mining-method to alleviate rockburst hazards.* In *Rockbursts and Seismicity in Mines* (Proc. 2nd Int. Symp. Rockbursts and Seismicity in Mines, Minneapolis, MN, June 8–10, 1988) (Balkema, Rotterdam 1990) pp. 349–353.

(Received October 6, 1992, revised March 8, 1993, accepted March 24, 1993)